Available online at www.sciencedirect.com

ScienceDirect

Procedia CIRP 117 (2023) 205–210

www.elsevier.com/locate/procedia

19th CIRP Conference on Modeling of Machining Operations

3D FEM heat transfer simulation of surface grinding of cryogenic pre-cooled parts

D. Weber[a]*, B. Kirsch[a], J.S. Silva[b], E.J. da Silva[b], J.C. Aurich[a]

[a]*Institute for Manufacturing Technology and Production Systems, RPTU in Kaiserslautern, Gottlieb-Daimler-Str., 67663 Kaiserslautern, Germany*
[b]*Department of Production Engineering, Laboratory for Advanced Processes and Sustainability, University of São Paulo, 13566-590, São Carlos, SP, Brazil*

* Corresponding author. Tel.: +49-631-205-5911. *E-mail address:* daniel.weber@mv.uni-kl.de

Abstract

Cooling lubricants are used in grinding to minimize heat-related problems such as surface cracks, burn and tensile residual stresses. An alternative is the cryogenic cooling, where the cryogenics like LN_2 are supplied at very low temperatures. The feasibility of different cryogenic cooling strategies depends on the workpiece volume-to-surface ratio. In this study 3D FEM heat transfer simulations are presented, which map the temporal and spatial temperature development, to assess the potential of LN_2 pre-cooling when dry surface grinding. Different clamping strategies in terms of insulation are investigated simulatively and experimentally.
It could be shown that clamping covers are required to maintain the cryogenic temperature in the workpiece during surface grinding due to their sufficient insulation. The temperatures during grinding of pre-cooled workpieces were successfully predicted by the developed FEM heat transfer simulation model.

Keywords: Type your keywords here, separated by semicolons ;

1. Introduction

Grinding is often used as a finishing process at the end of the value chain. The application of metal working fluids (MWF) minimizes heat-associated problems such as surface cracks, workpiece surface burn and tensile residual stresses, and therefore increases the workpiece quality [1]. However, MWF are a significant cost factor due to their acquisition cost, supply costs, filtration, recycling, and disposal. Possible alternatives are biodegradable coolants, minimum quantity lubrication (MQL), which is characterized by the supply as spray or mist, and cryogenic or dry machining [2]. Major drawbacks of MQL compared to conventional cooling are lower removal rates as well as higher surface roughness and thermally damaged surfaces [3, 4]. In contrast, cryogenic machining, which is usually characterized by the application of a cold high-speed gas jet (usually CO_2 or LN_2), showed significant improvements in the form of a reduction of tensile residual stresses, plastic deformations, microcracking and oxidation [5]. Thus, higher removal rates could be achieved compared to conventional MWF without thermally damaging the workpiece [6, 7]. Another advantage is the inert nature and immediate evaporation of the cryogenic substances from the environment, which avoids costs related to recycling and disposal. The majority of the studies in this field is confined to in-process cryogenic cooling. It was found that this strategy enhanced the bond strength of the grinding wheel, which increased the G-ratio, but also had an adverse effect on the grindability in terms of retaining worn out grits which resulted in a higher spindle power consumption [8]. Moreover, for the in-process application of cryogenics, the additional cost of the cryogenic delivery system and safety requirements to the operator are disadvantages. Therefore, in recent attempts the cryogenic pre-cooling, in which heat is extracted from the workpiece prior to grinding, was investigated [9]. In external cylindrical plunge grinding of AISI 1045, cryogenic pre-

10.1016/j.procir.2023.03.036

cooling achieved better surface finish, no thermal damage and no white layers, compared to conventional cooling [9]. However, according to Oliveira et al., the success of this cooling method depends on the amount of heat that can be extracted from the workpiece during the pre-cooling phase. This amount should be approximately equal to the total heat generated during grinding by convection, chip formation, plowing and rubbing of abrasive grains [9]. This in turn, and therefore the temperatures in the workpiece, depends on the workpiece dimension [9]. In particular, the surface-to-volume ratio (A/V ratio) influences the heat absorption or dissipation by convection. However, the dissipated heat due to the clamping strategy and their effect on the workpiece temperature evolution have not been considered yet.

3D heat transfer simulations based on the finite element method (FEM) offer the possibility of the temporal and local mapping of the temperature development in the workpiece and thus form the basis for assessing the suitability of the described cryogenic cooling strategies during grinding [9]. For example, Oliveira et al. were able to predict the workpiece temperatures of an AISI 1045 shaft pre-cooled to -85 °C (100 s in LN_2) during external cylindrical plunge grinding [9].

Our previously developed 3D FEM heat transfer model, which simplifies the grinding process in terms of a moving heat source, was successfully applied for dry surface grinding [10]. The focus of this paper is to extend the model by the cryogenic pre-cooling to investigate its ability for surface grinding. Another objective is to determine the effect of the clamping strategy in regard to a successful application of the cryogenic pre-cooling method. The simulation model is validated by measured temperatures during surface grinding experiments of pre-cooled workpieces.

Nomenclature

a_e	depth of cut
a_{ed}	dressing depth of cut
b	workpiece width
D	diameter of wheel
F_n	normal force
F_t	tangential force
h	convective heat transfer (film) coefficient
k	thermal conductance
l_c	contact length
P	grinding power
q_w	heat flux per unit area into workpiece
Q_w	material removal rate
T_B	bulk temperature
T_{BE}	bulk temperature at end of grinding step
T_S	(near) surface temperature
T_u	surrounding temperature
T_0	initial temperature
u	specific grinding energy
u_{ch}	specific grinding energy of chip formation
U_d	dressing overlap ratio
v_c	cutting speed
v_d	dressing feed speed
v_s	grinding wheel circumferential speed
v_w	workpiece speed
ε	energy partition

2. Methods

2.1. Experiments

Up-grinding was carried out on workpieces made of hardened and tempered steel AISI 4140H (42CrMo4; 40 ± 4 HRC) of the dimensions 125x19.3x23.2 mm^3 (V/A= 4.9 mm) on the ELB CAM-Master I/1 FR[1]. A vitrified bonded corundum grinding wheel with a diameter D of 400 mm (400x22x127 EKSP/EKW 60/1 I 6 V5900) was used. Three different workpiece velocities v_w (1; 2; 6 m/min), which resulted in different thermal loads, were investigated at a constant grinding wheel circumferential speed v_s of 30 m/s for grinding of pre-cooled workpieces. Multiple consecutive grinding steps with a depth of cut a_e of 25 µm were carried out. To investigate the effect of the insulation of the clamping on the thermal behavior of the workpiece, three different clamping strategies were investigated (see Fig. 1):

- vise as is (without cover; material jaws: 42CrMo4)
- vise with 3 mm fiberglass (glass-reinforced plastic: GRP) cover
- vise with 7 mm polyurethane (PUR) cover

Pre-cooling the workpiece was firstly attempted by leaving it in a dewar, filled with liquid LN_2, till a body temperature of -196 °C was reached. However, initial tests showed that, independent of the clamping strategy, the time prior to grinding, containing the clamping and the z-axis zero-point determination of the workpiece, was too long. This led to a heating of the workpiece to room temperature even before the actual surface grinding steps with a constant depth of cut of 25 µm took place. Therefore, an alternative set-up was used: After clamping the workpiece and zero-point determination, the top third of the workpiece, which protruded the vise, was cooled down in liquid LN_2 with the help of a styrofoam container (see Fig. 1). For the GRP cover the workpiece was pre-cooled 15 min in liquid LN_2 to reach a cryogenic temperature of -190 °C, 10 min respectively for the PUR cover. About -175 °C were left in the workpiece by the time the styrofoam container was removed. The workpieces were pre-ground (> 100 µm) to flatten the part prior to pre-cooling

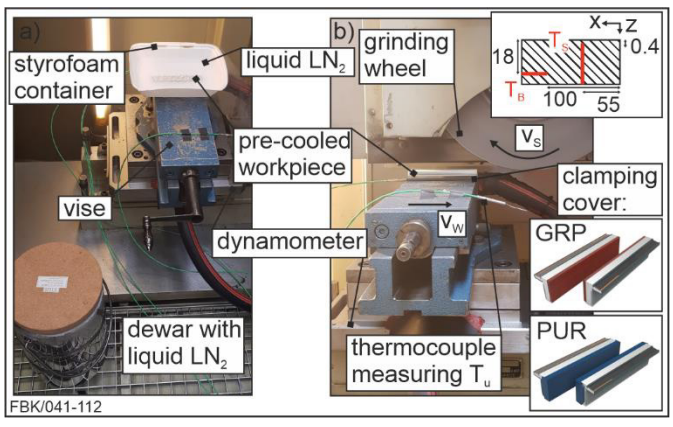

Fig. 1. (a) Pre-cooling of workpiece; (b) grinding of pre-cooled workpiece

Dressing of the grinding wheel was done prior to grinding each workpiece with an overlap ratio of U_d=7 (v_d=350 mm/min, a_{ed}=0,02 mm) to enable high temperatures during grinding operation.

The temperatures were measured continuously by means of two thermocouples (D_T=1 mm) for the pre-cooling and grinding process. One in the (near) surface area of the workpiece (T_S: z=400 µm, x=55 mm; y=9.65 mm, see Fig. 1) and one thermocouple at a greater distance from the surface, measuring the temperature in the bulk (T_B: z=18 mm; x=100 mm; y=9.65 mm, see Fig. 1) with a sampling rate of 100 Hz. The thermocouples were inserted by means of eroded holes (D_{edm} = 1.3 mm) on the workpiece bottom (T_S), the left side respectively (T_B), see Fig. 1. Multiple grinding steps were performed until the exposure of the eroded hole with the thermocouple T_S inside. As many consecutive cuts were executed for the pre-cooled workpieces until room temperature T_u was reached. This procedure was repeated until the thermocouple T_S was exposed. As a characteristic value $\Delta T_S = T_{S,max}$-$T_{S,min}$ was calculated for each single cut.

In addition to the temperatures, the forces (normal force, tangential force) were recorded using a dynamometer. The steady state (80% of the signal without cut-in and cut-out effects) was analyzed by arithmetic averaging (see Fig 2).

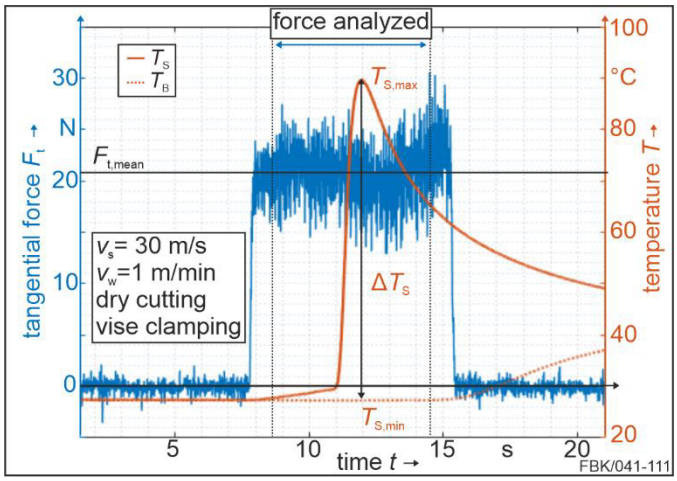

Fig. 2. example of force (low pass filter 50 Hz) and temperature signal

2.2. Simulation

A dynamic 3D FEM heat transfer model was built in ABAQUS[1] to simulate the temperature field when surface grinding. Besides the workpiece, a part of the clamping fixture, clamping cover respectively, was also considered to account for the heat transfer between both bodies (see Fig. 3).

Table 1. material data

	density ρ in kg/m³	specific heat capacity c in J/(kg°C)	thermal conduction h in W/(m°C)
42CrMo4	7850	486	42.6
PUR	1200	1760	0.58
GPR	2000	1200	0.6

Due to the existing symmetry in the orthogonal feed direction, only one half of the clamped workpiece was modeled. To avoid modeling the entire vise, the assumption was made that the temperature at the end of the clamping covers corresponds to the surrounding temperature Tu. The material data of the workpiece and clamping fixture (42CrMo4), clamping cover (GRP, PUR) respectively, is shown in Table 1.

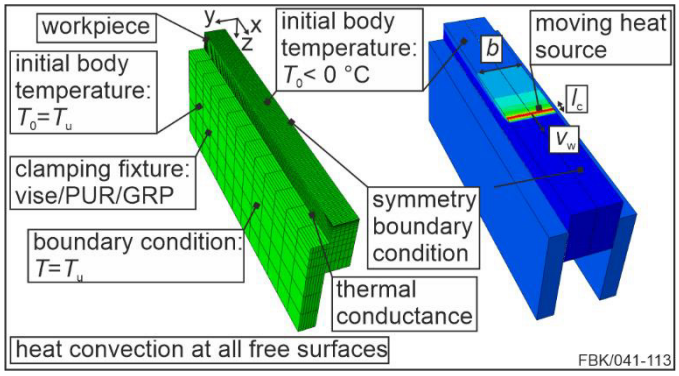

Fig. 3. FEM simulation model: moving surface heat flux

The mesh consists of 21,000 elements (workpiece) and 637/ 1,350/ 637 elements (clamping fixture/ GRP/ PUR) of the type DC3D8. The workpiece element length was chosen to 0.5 mm (x-) and 1.5 mm (y-direction). It was refined near the machined surface in z-direction (0.1 mm) to resolve the temperature gradient sufficiently and coarsened in the opposite direction (5 mm) to reduce the number of elements to save computational time. The heat input from grinding was modeled via the moving surface heat flux command (ABAQUS subroutine DFLUX). Its speed corresponded to the respective workpiece speed v_w. The surface heat flux q_w (heat flux per area) was used as an input and calculated via the measured tangential force, see Eq. (1) [11,12].

$$q_w = \frac{\varepsilon P}{l_c b} \quad \text{with} \quad P = F_t \cdot v_c \quad \text{and} \quad l_c = \sqrt{a_e \cdot D} \quad (1)$$

The energy partition ε can be calculated with Eq. (2) and usually varies between 60 to 90% when grinding steels using grinding wheels with conventional aluminum oxide grits [11,12].

$$\varepsilon = \frac{u - 0.45 u_{ch}}{u} \quad \text{with} \quad u = \frac{P}{Q_w} \quad \text{and} \quad u_{ch}=13.8\ \text{J/mm}^3 \quad (2)$$

In general, the heat can be emitted by conduction, convection or radiation. In this model, heat dissipation by radiation is neglected. The applied temperature-dependent heat transfer coefficient by convection h was determined in previous investigations, where a workpiece was heated to +170 °C (cooled down to -170 °C in liquid LN_2) and cooled (heated) at the surrounding air [10]. Furthermore, the thermal conductivity k between the workpiece and the clamping fixture, covers respectively, was determined according to the experiments described in [10]: The workpiece was clamped after heating (cooling) it to +80 °C (-170 °C) and the temperature of the cooling (heating) process was measured at the bulk location T_B. A similar model as described before (without moving heat flux) with a matching initial temperature of the workpiece was set up. The temperature dependent thermal conductance k was then determined by a parameter variation and an iterative comparison of the predicted temperature curve with measured data. Meaning

that in a first step *k(T)* was assumed and then successively adjusted to the measured temperature curve.

3. Results

3.1. Determination of the thermal conductance k

The measured bulk temperatures T_B are plotted over time in Fig. 4 for the heating and cooling processes of the workpiece clamped in different covers (without grinding). It is visible that the PUR cover leads to the best insulation, keeping the cryogenic temperatures the longest in the workpiece, followed by the GRP cover. Furthermore, the derived values for the temperature dependent thermal conductance *k* are given in Table 2 for each clamping strategy and the simulated temperatures T_B for the cooling and heating process based on those values are plotted in Fig 4.

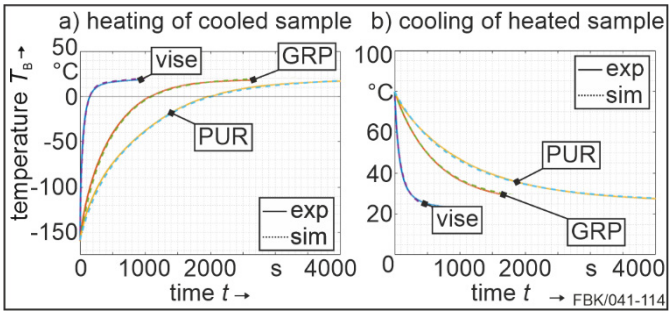

Fig. 4. determination of thermal conductance *k* for different clamping covers

Table 2. thermal conductance *k* in W/(m²°C)

temperature in °C	42CrMo4 -vise (42CrMo4)	42CrMo4 -GPR cover	42CrMo4 -PUR cover
-170	9000	200	120
-160	9000	180	100
-120	8500	150	70
-80	8500	140	55
-40	8000	130	38
0	3000	90	25
+20	50	60	5
+60	3500	80	40
+100	5500	150	70

3.2. Experimental results: Clamping cover comparison

Fig. 5 exemplarily shows the measured tangential force F_t and temperatures T_S and T_B of multiple consecutive grinding steps for a pre-cooled and not cooled workpiece. Even though the surface was ground flat before, the first three grinding cuts do not have a constant depth of cut of 25 µm. Mostly for the first and second grinding step, only the areas close to the edges of the workpiece, at the beginning and end of a cut, were ground with lower forces measured. Whereas at the following step (cut 3) only material in the middle was ground (see Fig 5) with higher forces measured. After those cuts a more stable cutting with similar measured forces is observed. This effect is evident for all investigated workpiece velocities and independent of the cooling strategy (with or without pre-cooling). One possible explanation is that due to prior cuts and their induced heat an uneven expansion and contraction of the workpiece happened, which led to an uneven surface of the workpiece.

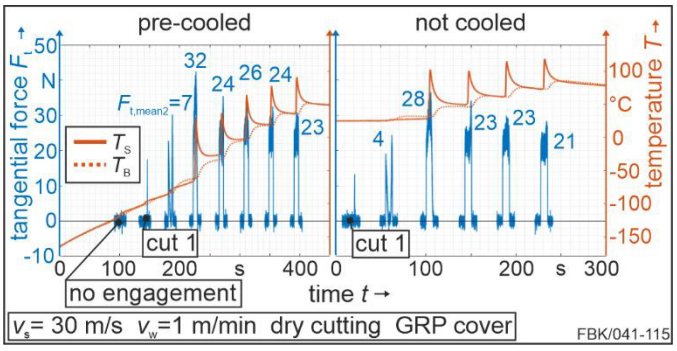

Fig. 5. measured forces and temperatures

Furthermore, the forces are higher at cryogenic temperatures, because of the higher temperature difference between two consecutive cuts (higher temperature gradient), which led to a higher expansion of the workpiece and therefore to higher cut depths than 25 µm. For example, a temperature difference of 50 °C leads to an expansion of an 8 mm long 42CrMo4 workpiece (corresponding to the protruding workpiece height) (α=13E-6 1/K) by 5.2 µm, which is significant compared to the low depth of cut. Furthermore, due to the reduced thermal load within the surface layer, the dynamic recrystallization is suppressed more efficiently promoting strain hardening, leading to the deterioration of the thermal softening [13].

For using the vise without any clamping cover only an initial temperature of -40 °C was achieved (10 min of pre-cooling) due to the high thermal conductance of the vise. Although z-zero was determined prior to pre-cooling, a certain time passed until the first cut with a constant depth was made. Due to the high thermal conductance of the vise, the pre-cooled workpiece heated up so fast that it reached room temperature before the actual grinding with a constant depth of cut could happen (see Fig. 6). Therefore, a clamping cover had to be used to achieve and maintain a sufficient cryogenic temperature during grinding.

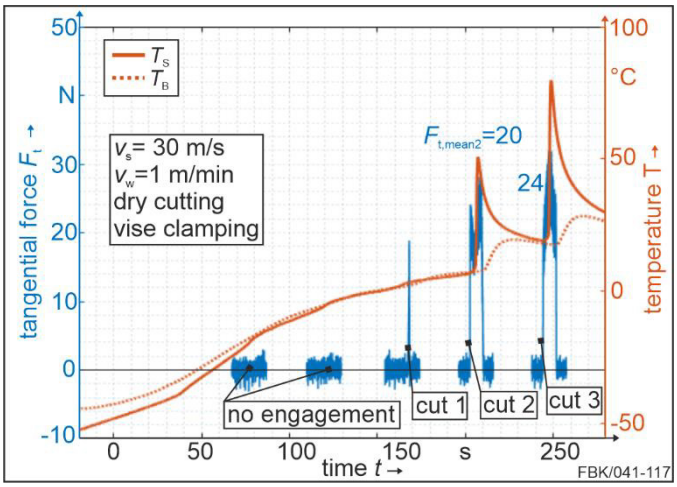

Fig. 6. measured forces of pre-cooled workpiece in vise without any cover

Table 3 shows the comparison of the clamping strategies for each workpiece speed, including the number of cuts with a constant a_e=25 µm (not included 3 to 4 cuts with lower depth at the beginning) which were achieved until room temperature T_u was reached, the arithmetic mean of F_n and F_t ($F_{n,mean}$, $F_{t,mean}$, averaged over the number of consecutive cuts with a_e=25 µm), the calculated heat input and the arithmetic mean of ΔT_S ($\Delta T_{S,mean}$, averaged over the number of consecutive cuts with a_e=25 µm). For an increased workpiece speed, the process time for one cut was shortened, which means that more cuts were achieved until room temperature was reached. Also, as the workpiece speed increased, the forces increased and with them the heat flux due to an increased material removal rate. Measured forces were at a similar level for the same workpiece speed and different clamping covers, but a trend is evident with slightly higher forces for the PUR cover (except for v_w=2 m/min). This could be attributed to the fact that the PUR cover kept the cryogenic temperatures longer in the workpieces, resulting in more cuts at lower temperatures. But in general, it must be considered, that a certain variation of the forces when using the same parameters were evident for dry grinding due to the fast tool wear (clogging of the wheel) [12]. Higher forces for the same v_w also led to higher temperature differences ΔT_S, due to the increased power, or heat input respectively (see Eq. 1).

Table 3. Comparison of different clamping strategies

v_w in m/min	cover	cut *	$F_{n,mean}$ in N	$F_{t,mean}$ in N	q_w in MW/m²	$\Delta T_{S,mean}$ in °C
1	GRP	2	37±1.3	25±1.5	11.7±0.8	65±1.9
1	PUR	3	48±1.2	31±0.3	14.9±0.2	98±10.4
2	GRP	4	76±6.2	48±3.1	22.7±1.5	82±11.8
2	PUR	5	68±12.8	44±8.8	20.4±4.4	73±6.3
6	GRP	8	115±5.5	66±2.1	28.2±1.1	41±2.8
6	PUR	8	131±2.2	74±1.0	32.3±0.5	55±3.0

** Number of cuts in total with constant depth of cut a_e=25µm*

3.3. Comparison of experiments and simulation

Fig.7 exemplarily shows the comparison of the simulated and measured temperatures for the workpiece ground with v_w=6 m/min and clamped in the PUR covers. For this example, in total 12 cuts were made, where a constant depth of cut was reached after the 4th cut. The first two cuts were not considered in the simulation, because they only ground a small portion at end of the workpiece.

Table 4 highlights, analogous to the characteristic values from Table 3, the differences between model and experiment. In regions close to the surface (T_S) the deviations of the measured and simulated temperature were the highest for all investigated workpiece velocities and clamping strategies. Deviations up to 971 % were observed (see Table 4). This effect could be explained by inaccurate temperature measurements: The eroded holes are tapered at the tip and therefore do not have a flat face. This means that the measuring tip of the thermocouples may not have touched the workpiece over the entire surface. Although material was removed over the thermocouple tip, a narrow air gap remained. So, especially high temperature gradients in the near surface area cannot be fully resolved by the measurements. Additionally, the presence of the response time of the thermocouple deteriorates the accuracy of the measured maximum temperatures for high v_w. This fits the observation of increased deviations of measured and simulated temperatures for increased workpiece speeds v_w. Thus, it is to be expected that the actual surface temperatures in these regions were significantly higher than those measured. This also does not allow for a comparison of the measured temperatures among each other, because the remaining distance from the thermocouple tip to the grinding wheel could vary.

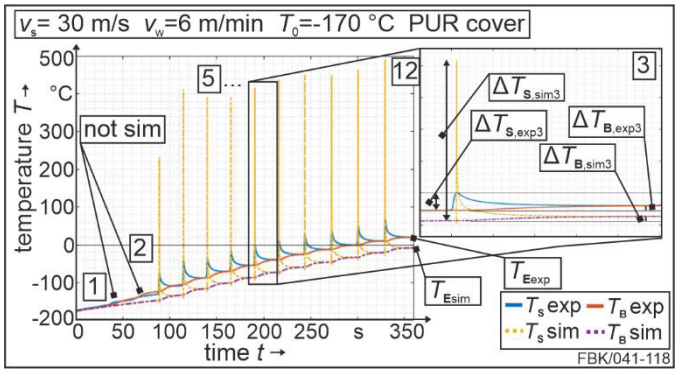

Fig. 7. measured and simulated temperatures of workpiece clamped in PUR cover (v_w=6 m/min)

Table 4. Comparison of experiment and simulation

	GRP 1 m/min	PUR 1 m/min	GRP 2 m/min	PUR 2 m/min	GRP 6 m/min	PUR 6 m/min
$\Delta T_{S,exp}$ in °C	65±2	98±10	82±12	73±6	41±3	55±3
$\Delta T_{S,sim}$ in °C	398±26	511±6	580±39	522±113	439±16	501±7
$(\Delta T_{S,sim} - \Delta T_{S,exp})/\Delta T_{S,exp}$	512 %	421 %	607 %	615 %	971 %	811 %
$\Delta T_{B,exp}$ in °C	25±4	29±6	23±5	21±4	13±4	13±3
$\Delta T_{B,sim}$ in °C	27±1	33±2	25±4	23±4	13±2	14±1
$(\Delta T_{B,sim} - \Delta T_{B,exp})/\Delta T_{B,exp}$	8 %	14 %	9 %	10 %	0 %	8 %
$T_{BE,exp}$ in °C	17	23	26	19	23	20
$T_{BE,sim}$ in °C	15	23	32	15	5	-8
$(\Delta T_{BE,sim} - T_{BE,exp})/\Delta T_{BE,exp}$	-12 %	0 %	23 %	-21 %	-78 %	-140 %

The temperatures in deeper regions (T_B) are predicted with a higher accuracy, because here temperature gradients are significant lower. Deviations between simulation and experiment were smaller than 14 % (see Table 4), which indicates that the characteristics of the model (heat flux input and thermal properties) were chosen appropriate. However, a deviation at the end of the measurements (when room temperature T_u is reached) was evident (T_E). This is mainly due to the mentioned first 3 to 4 cuts with inconstant a_e. Since the heat input relies on the arithmetic mean of the tangential force per cut, an uneven force distribution leading to an uneven heat input is not represented by the model. If only the temperatures for cuts with constant a_e=25 µm were simulated, the accuracy of T_B and T_E is even higher (see Fig. 8).

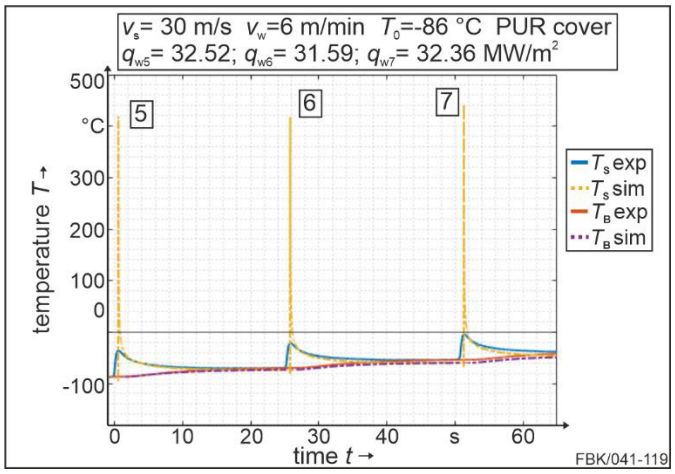

Fig. 8. measured and simulated temperatures of cut 5 to 7 of workpiece clamped in PUR cover (v_w=6 m/min)

To further investigate the true surface temperature, more grinding steps were experimentally carried out until the thermocouple was fully exposed (v_w= 6 m/min, PUR cover). This led to the grinding of the thermocouple face and its destruction. However, the surface temperature measurement directly prior to the destruction was recorded and is highlighted in Fig. 9. The measured maximum surface temperature (482 °C) almost matches the simulated one (497 °C), proving the quality of the simulation.

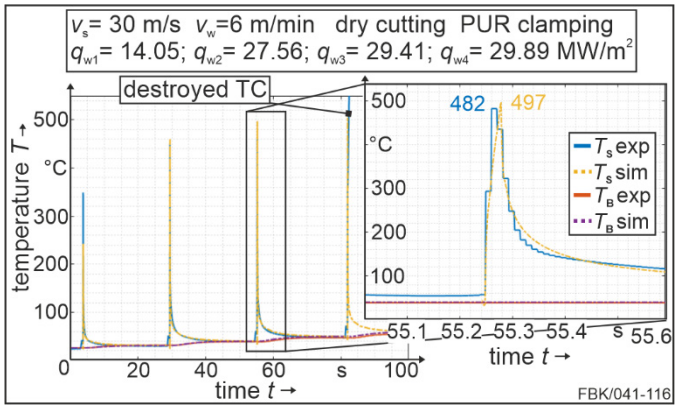

Fig. 9. measured and simulated temperatures at fully exposed thermocouple

4. Conclusion and summary

The following conclusions can be drawn: Clamping covers must be used for a successful application of the cryogenic pre-cooling method for surface grinding, because of their sufficient insulation. In general, pre-cooling must happen after clamping the workpiece, to save time, in which the workpiece would heat up. The pre-cooling method is not ideal for surface grinding with low depths of cut, because of the high temperature differences in between two cuts (especially at cryogenic temperatures). The expansion of the workpiece is relatively high compared to an a_e of 25 µm. Therefore, higher depths of cut will be investigated in the future.

In general, the developed simulation model is capable of predicting the temperatures for grinding pre-cooled workpieces with different clamping strategies. Large deviations between predicted and measured temperature data were found in the near surface area, where high temperature gradients appear. This was proven to be a measurement inaccuracy due to the combination of the presence of an air gap at the tip of the eroded holes and the response time of the thermocouple. Meaning that the true surface temperature is closer to the simulated one. Only small temperature deviations between measurement and simulation were found in the bulk of the workpiece. Uneven force distributions need to be considered in the future. Furthermore, the model will be used to predict whether pre-cooling can be used for different workpiece geometries (different V/A-ratios). Also, a method will be developed to predict the heat input, so that no measured forces are required anymore. Besides, the model will be extended to cylindrical plunge grinding.

Acknowledgements

The authors would like to thank the German Research Foundation (DFG) and the Fundação de Amparo à Pesquisa do Estado de São Paulo (FAPESP) for the financial support within the project AU 185/82-1 “Extending the possibilities of cryogenic assisted grinding” (FAPESP funding No. 2018/16416-5). [1]Naming of specific manufacturers is done solely for the sake of completeness and does not necessarily imply an endorsement of the named companies nor that the products are necessarily the best for the purpose.

References

[1] Yao C, Wang T, Xiao W, Huang X, Ren J. Experimental study on grinding force and grinding tem-perature of Aermet 100 steel in surface grinding. Journal of Materials Processing Technol 214 (2014), p. 2191–2199.
[2] Inasaki I, Tönshoff HK., Howes TD. Abrasive machining in the future. CIRP Annals – Manufactur-ing Technology 42 (1993), p. 723–732.
[3] Barczak LM, Batako ADL, Morgan MN. A study of plane surface grinding under minimum quanti-ty lubrication (MQL) conditions. Int Journal of Machine Tools and Manufacture 50 (2010), p. 977–985.
[4] Weinert K, Inasaki I, Sutherland JW, Wakabayashi T. Dry machining and minimum quantity lubrication. CIRP Annals - Manufacturing Technology 53 (2004), p. 511–537.
[5] Chattopadhyay AB, Bose A, Chattopdhyay AK. Improvements in grinding steels by cryogenic cool-ing. Precision Engineering 7 (1985), p. 93–98.
[6] Paul S, Chattopadhyay AB. The effect of cryogenic cooling on grinding forces. International Journal of Machine Tools and Manufacture 36 (1996), p. 63–72.
[7] Ramesh K, Yeob SH, Zhong ZW, Huang H. Ecological grinding with chilled air as coolant. Proceed-ings of the Institution of Mechanical Engineers, Part B: Journal of Engineering Manufacture 217 (2003), p. 409–419.
[8] Reddy PP, Ghosh A. Some critical issues in cryo-grinding by a vitrified bonded alumina wheel using liquid nitrogen jet. Journal of Materials Processing Technology 229 (2016), p. 329–337.
[9] Oliveira JFG., Silva EJ, Coelho RT, Brozek L, Bottene AC, Marcos GP. Dry grinding process with workpiece precooling. CIRP Annals - Manufacturing Technology 64 (2015), p. 329–332.
[10] Weber D, Kirsch B, da Silva EJ, Aurich, JC. 3D FEM Wärmeübertragungssimulation des Schleifens. ZWF - Zeitschrift für wirtschaftlichen Fabrikbetrieb 117/7-8 (2022), p. 484-488.
[11] Malkin S, Guo C. Thermal Analysis of Grinding. CIRP Annals 56\2 (2007), p. 760-782.
[12] Malkin S, Guo C. Grinding Technology: Theory and application of machining with abrasives. Industrial Press, Inc. 2nd Ed. (2008).
[13] Jawahir IS, Attia H, Biermann D, Duflou J, Klocke F, Meyer D, Newman ST, Pusavec F, Putz M, Rech J, Schulze V, Umbrello D. Cryogenic manufacturing processes. CIRP annals 65/2 (2016), p. 713-736.